

Fuel Slosh in a Motorcycle Tank

J. M. Sicilian and C. W. Hirt  
 Flow Science, Inc.  
 January 1989

Iwamoto and Nakano [1] have published experimental results that demonstrate the slosh of fuel in a motorcycle undergoing a rapid acceleration similar to what might be encountered in a crash. To simplify visual data recording, and subsequent analysis, the tests were conducted using rectangular tanks with clear side panels. A hydraulic generator was used to supply a half-sine-wave acceleration history to the tank. Pressures were measured at various locations along the walls of the tank.

This report presents computer simulations performed using FLOW-3D [2] of similar slosh experiments. The calculations simulated a half-sine-wave acceleration history (of 90 ms duration whose maximum amplitude is 35 G) applied to a rectangular container measuring 400 mm by 261 mm. (The transverse dimension was 243 mm.) Three pressure measurement locations were considered, as shown in Fig. 1.

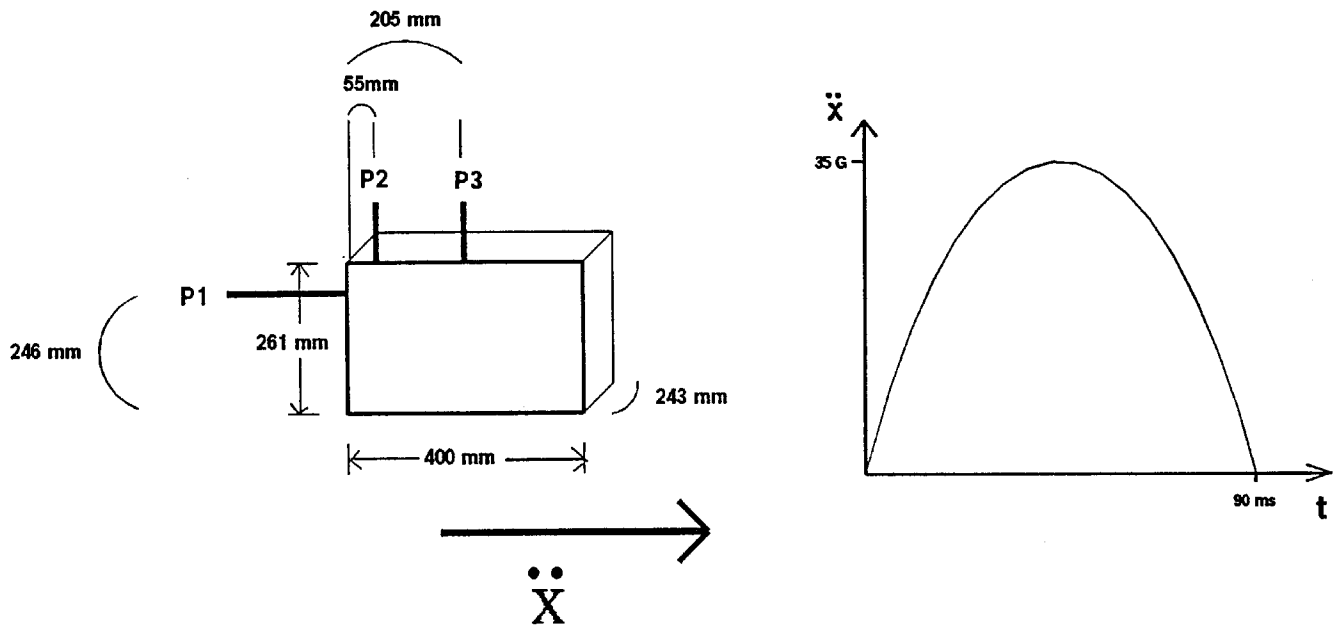


Fig. 1. Physical Tank Setup

Two fill levels were considered. The first (called 100% Fill) began with fluid to a height of 226 mm. (Motorcycle tanks always contain some void space to accommodate thermal expansion.) The second (75% Fill) case was filled to a height of 170 mm. The working fluid is gasoline ( $\rho=0.71$  gm/cc,  $\mu=4.9 \times 10^{-5}$  gm/cm/s).

### Computational Model

The FLOW-3D computations were performed in two-dimensional geometry. (As discussed below, the influence of wall shear was found to be small, even including turbulence effects.) As is usual with FLOW-3D, the calculations were performed in a reference frame which accelerates with the tank. The primary calculations neglected viscous effects, but a comparison computation was performed using a two-equation turbulence model to investigate the influence of viscosity on the fluid behavior.

Figure 2 shows the computational mesh used for all the FLOW-3D calculations. Smaller cells were located near the top and side walls since we anticipated the formation of thin sheets of fluid along these walls. Results presented for computed pressures and fluid fractions are located at the center of the cells indicated in Fig. 2. Note that the cell centers are somewhat removed from the wall. The centers are also slightly offset from the sensor locations parallel to the wall. While this offset could have been corrected by adjusting the mesh, very little change in results is expected from such minor changes.

Figure 3 displays the entire input file for the 100% Fill Case. We chose to use cgs units for these calculations. Therefore, the acceleration is given by

$$\ddot{x} = 34300 \sin(34.907 t)$$

where  $\ddot{x}$  is in  $\text{cm/s}^2$  and  $t$  is in seconds. These values are entered in NAMELIST MOTN which relies on the standard FLOW-3D acceleration history

$$\ddot{x} = A0 \sin(OMGO t)$$

Therefore, it was not necessary to modify the reference frame routine (MOTION) to perform these simulations.

## Results

Figures 4 and 5 display the fluid configurations and velocities for the inviscid 100% Fill and 75% Fill Cases, respectively. The gross fluid motion agrees well with that reported in Reference 1, although the details are influenced by the change in geometry and acceleration.

The calculated cell pressures near sensors P1, P2 and P3 are compared in Figs. 6 and 7 for the two fill levels. These pressures are static values and may not be directly comparable to the measurements reported in [1]. The dynamic contribution to the pressure [ $\rho u^2/2$ ] is similar in magnitude and can affect the reading on some types of sensors. Nonetheless, several trends described in Ref. 1 can be seen in the computed results. As one might expect, the sensors show a sequential wetting and corresponding pressure increase as the slosh front progresses from P1 to P2 to P3. Figure 8 shows computed values of fluid fraction rising abruptly as the slosh front reaches each location.

One feature that does not appear in the computed pressure history that was observed in the experiments is a secondary pressure peak. These secondary peaks were most prevalent for the 100% fill level at locations analogous to P1. The difference may be related to the different geometry and acceleration used in the simulations. Alternatively, some phenomena not included in the simulation may be the cause. Unresolved free surface waves in the fluid or structural response of the tank could explain the difference as could some transducer effects. Since the fluid motion seems to agree well, we believe that the hydraulics of our simulations are accurate.

Finally, the shape of the pressure pulse at P3 for the 75% case is quite different in these simulations from the experimental results. A typical pressure contour plot (Fig. 9) shows a nearly hydrostatic distribution (due to the acceleration) with P3 located close to the low pressure contour. A high pressure region in the top right corner indicates the turning of the slosh front through this corner at about this time.

An interesting phenomena appears if we compare the forces generated in these two cases. At first, one might expect the forces to be larger for the 100% Fill Case since it contains a larger mass of fluid. However, as can be inferred from Fig. 10, the larger time available for fluid to accelerate unimpeded leads to higher z-direction forces for the 75% Fill Case. Figure 11 supports this analysis, reporting that the kinetic energy of the fluid (and therefore its momentum) is significantly larger for

the lower fill level. To understand Fig. 10, consider the z momentum of the fluid. Initially, the z momentum increases as the fluid sloshes upward at the left side of the tank. To counter this, the tank experiences a negative z force. Later, when the fluid strikes the top, this z momentum must be reversed, at which time the container experiences a positive force. For the 100% Fill Case a second reversal of momentum occurs resulting in a second negative z-component force spike. The kinetic energy of the fluid does not show these reversals since it is not sensitive to the direction of flow.

### Turbulent Case

To investigate the influence of wall shear, viscosity and turbulence, the 75% fill simulation was repeated using FLOW-3D's k- turbulence model. (The Reynolds number for this flow is about  $6 \times 10^6$ .) A typical contour plot of the computed viscosity is shown in Fig. 12. There is a thin layer of high turbulent viscosity adjacent to the wall (in which  $\mu$  is approximately 100 to 1000 times the molecular value), but the bulk of the fluid experiences a nearly molecular viscosity. This has little influence on the fluid flow, as can be seen by comparing Fig. 13 with the 90.2 ms frame in Fig. 5 and Fig. 14 with Fig. 7.

### Computational Requirements

A total of 750 real computational cells were included in the mesh. The simulations were run on a MicroVAX II computer. Table I shows the CPU requirements of each calculation.

TABLE I  
CPU REQUIREMENTS for SIMULATIONS

<u>Case</u>	<u># Cycles</u>	<u>Total CPU</u>	<u>Average CPU/Cell/Cycle</u>
Inviscid 100% Fill	369	16,150 s	58 ms
Inviscid 75% Fill	291	9,945 s	46 ms
Turbulent 75% Fill	299	11,620 s	52 ms

These times are slightly higher than usually encountered with FLOW-3D because the continual change in acceleration causes the program to use many pressure iterations for each cycle of computation.

### Conclusions

FLOW-3D seems to predict reasonable slosh behavior for the cases simulated. Direct simulation of published results should allow more detailed evaluation of the program.

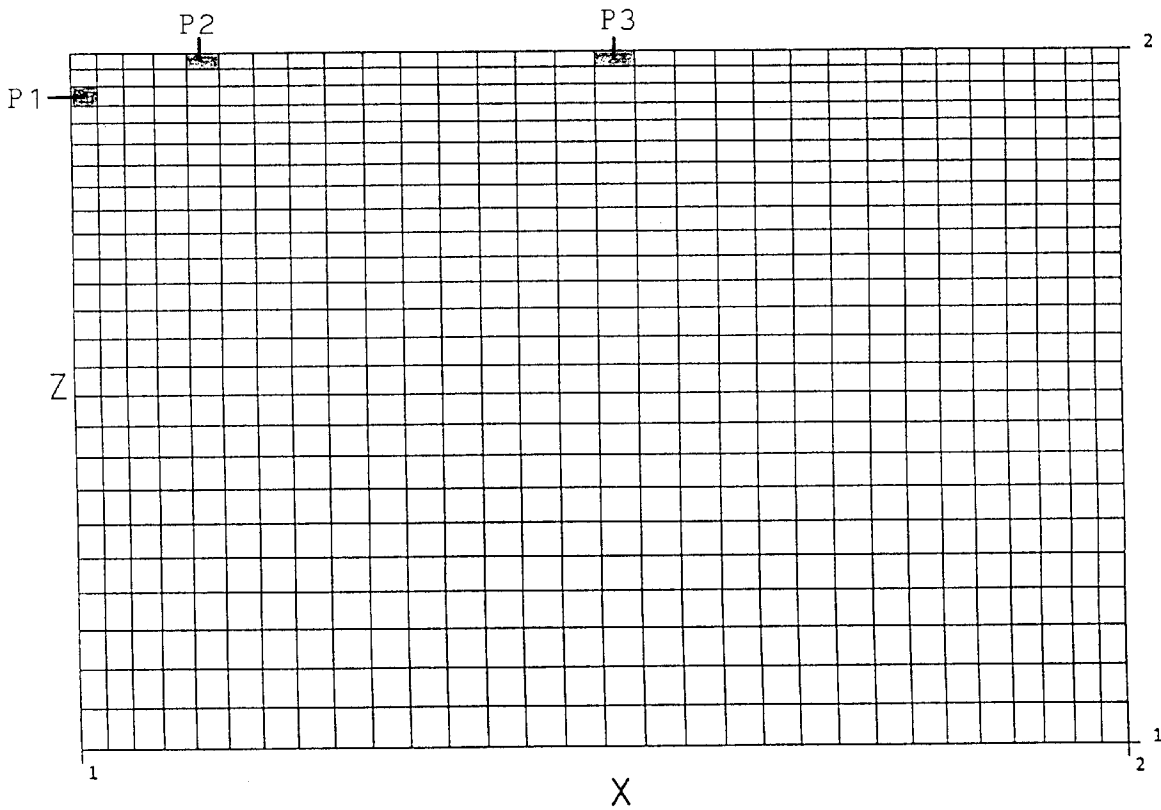
A more finely resolved computational mesh would probably improve some details of the results since the fluid compresses into a single cell layer at many times, particularly in the 75% Fill Case. Although this would be feasible in these two-dimensional simulations, it would create a more costly simulation if extended to three dimensions for the analysis of real fuel tank geometries. On the other hand, we believe the gross fluid motions and average forces should be quite good since the code closely conserves mass and momentum.

### References

- [1] Masatoshi Nakano and Tadamitsu Iwamoto, "Analysis of the Behavior of Liquid in a Fuel Tank," Society of Automotive Engineers,...
- [2] "FLOW-3D: Computational Modeling Power for Scientists and Engineers," Flow Science, Inc., report, (FSI-88-00-1) 1988.

# X-Z MESH

	X	Z
NUMBER OF CELLS=	30	25
SMALLEST CELL=	1.000E+00	6.000E-01
LARGEST CELL=	1.517E+00	1.488E+00
MAXIMUM CELL RATIO=	1.069E+00	1.062E+00
	AT CELL 2	AT CELL 25



PREP3D 15:38:10 9-JAN-89 MDXW PREP3D: VERSION 3, MOD 1, MVX 1988  
CRASH SLOSH - 100% - 35 G SINUSOID ACCELERATION - INVISID

Fig. 2. Computational Mesh

CRASH SLOSH - 100% - 35 G SINUSOID ACCELERATION - INVISID

```

$XPUT
  ITB=1,           IACCF=1,           IPDIS=1,
  RHOF=0.72,      GZ=-980.,           WL=2,
  WR=2,           WB=2,           WT=2,
  TWFIN=0.09,    DELT=0.001,        EPSI=0.1,
  PLTDT=0.005,   PRTDT=0.09,
$END
$MESH
  PX(2)=40.,      SIZEX(1)=1.0,      SIZEX(2)=1.0,
  NXCELT=30,
  PY(2)=24.3,     SIZEZ(2)=0.6,      NYCELT=1,
  PZ(2)=26.1,
$END
$OBS
$END
$FL
  FLHT=22.6,
$END
$BF
$END
$TEMP
$END
$MOTN
  A0=34300.,      OMG0=34.907,
$END
$GRAFIC
  NVPLTS=1,       NCPLTS=1,           NWINF=1,
  WINTL(1)='NEAR P1', ILOC(1)=2, JLOC(1)=2, KLOC(1)=24,
  WINTL(2)='NEAR P2', ILOC(2)=6, JLOC(2)=2, KLOC(2)=26,
  WINTL(3)='NEAR P3', ILOC(3)=17, JLOC(3)=2, KLOC(3)=26,
  WINTL(4)='TOP CORNER', ILOC(4)=31, JLOC(4)=2, KLOC(4)=26,
  WINTL(5)='BOTTOM CORNER', ILOC(5)=31, JLOC(5)=2, KLOC(5)=2,
$END
$PARTS
$END

```

Fig. 3. FLOW-3D Input File

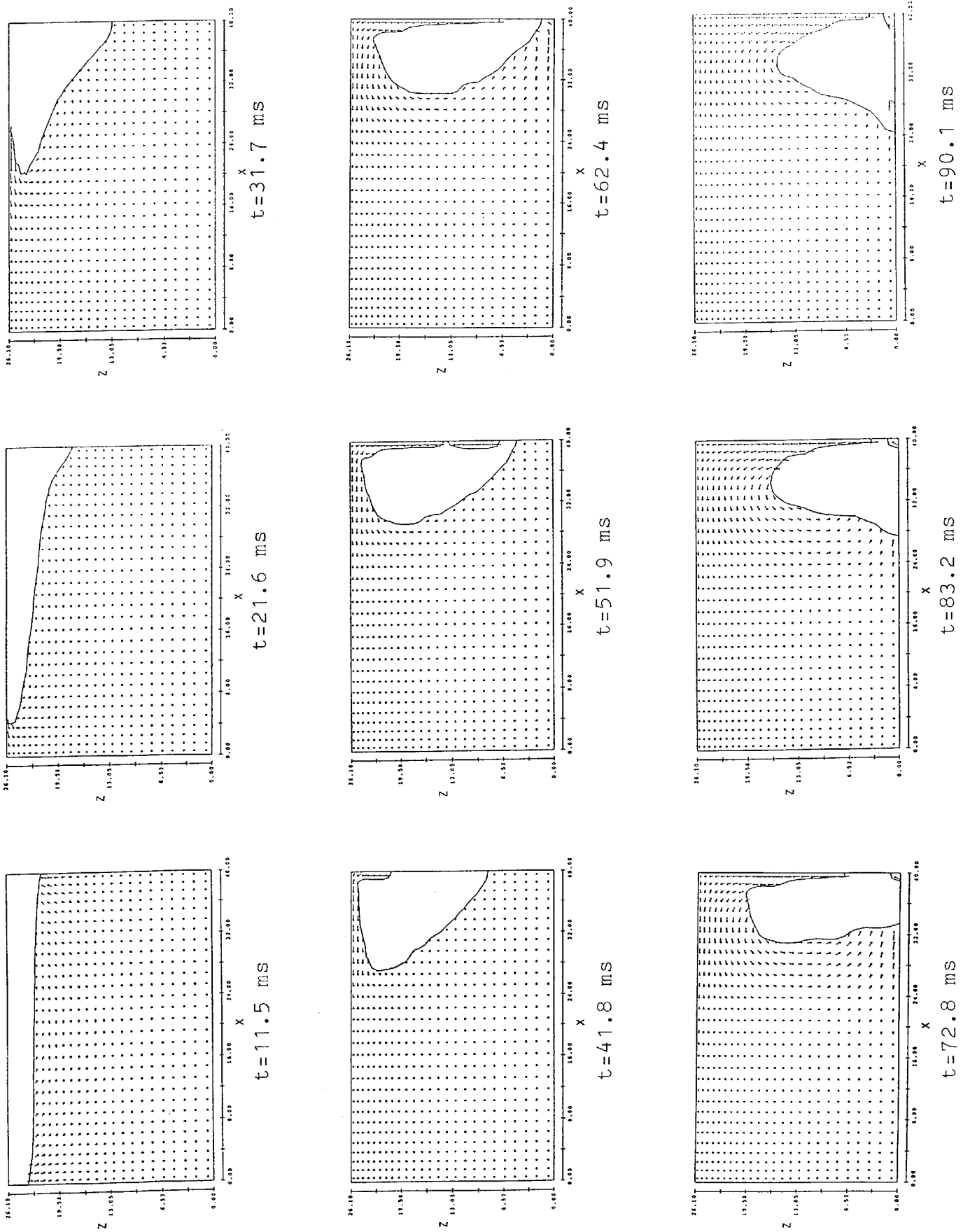


Fig. 4. Velocity and Free Surface Distributions for 100% Fill Case.

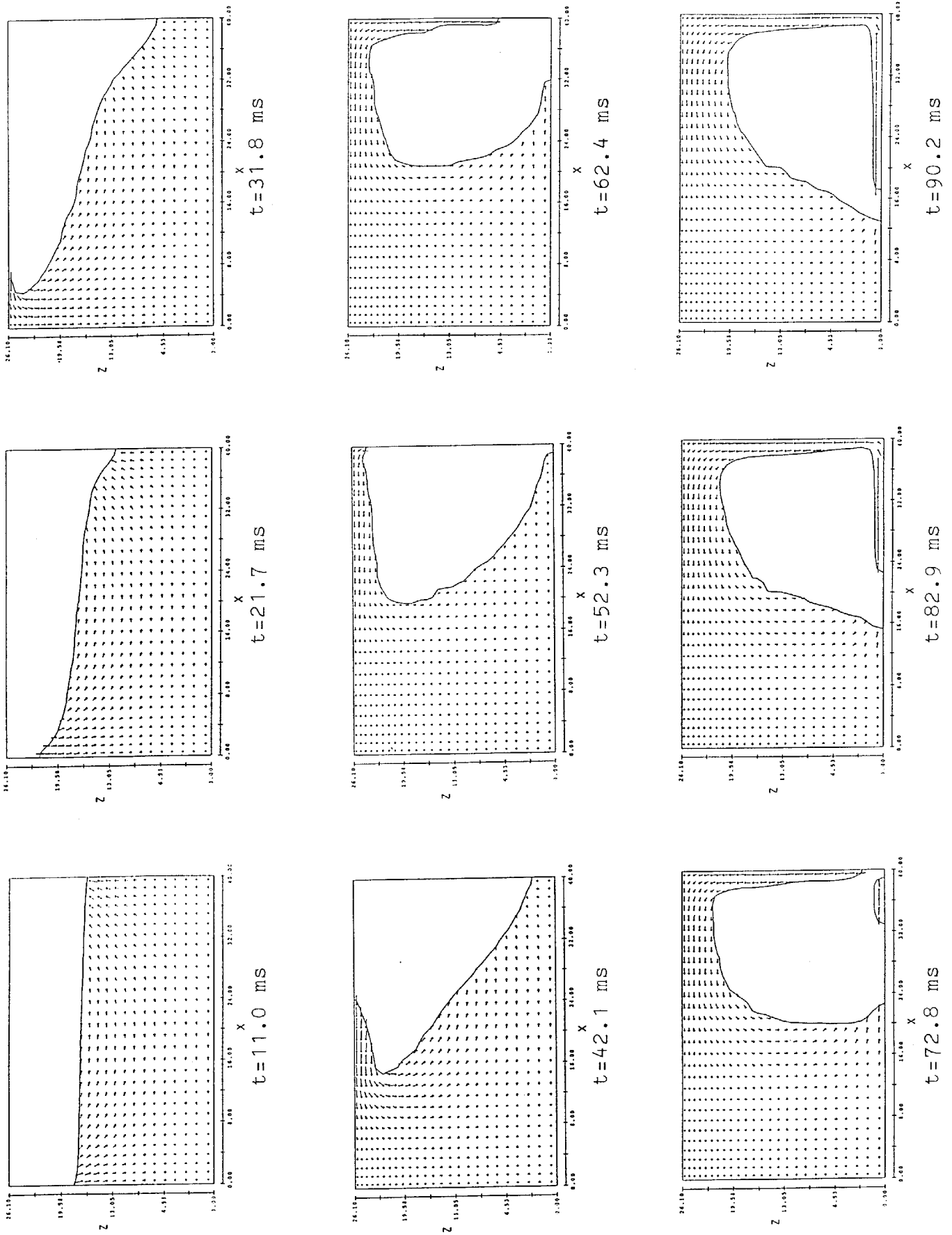
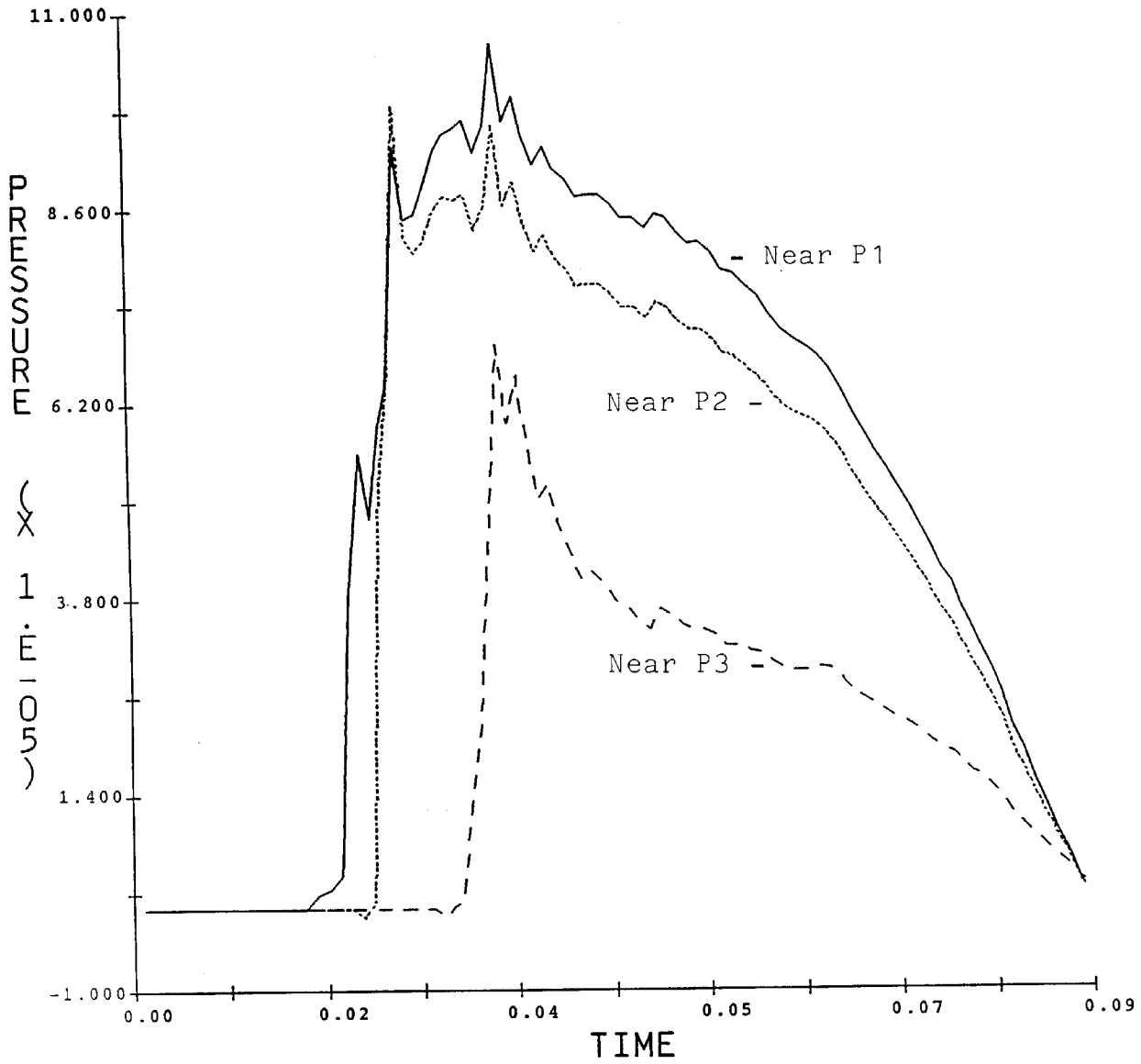


Fig. 5. Velocity and Free Surface Distributions for 75% Fill Case.

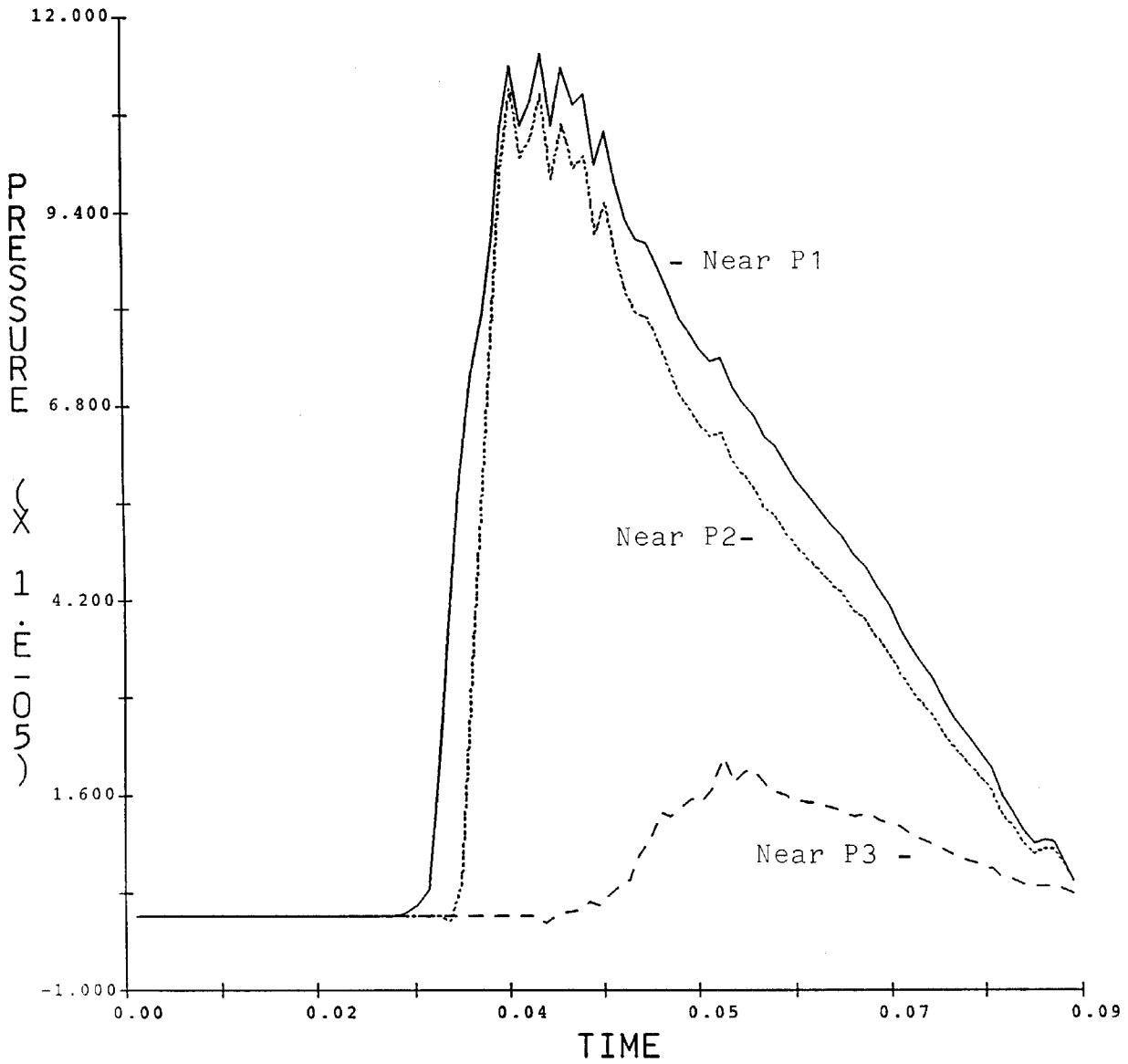
# PRESSURE COMPARISON



HYDR3D 17:36:14 6-JAN-89 FVNN VERSION 3, MOD 1, MVX 1988 X1= 2 X2= 2 X3= 24  
 CRASH SLOSH - 100% - 35 G SINUSOID ACCELERATION - INVISID

Fig. 6. Static Fluid Pressures at P1, P2, P3 for 100% Fill Case.

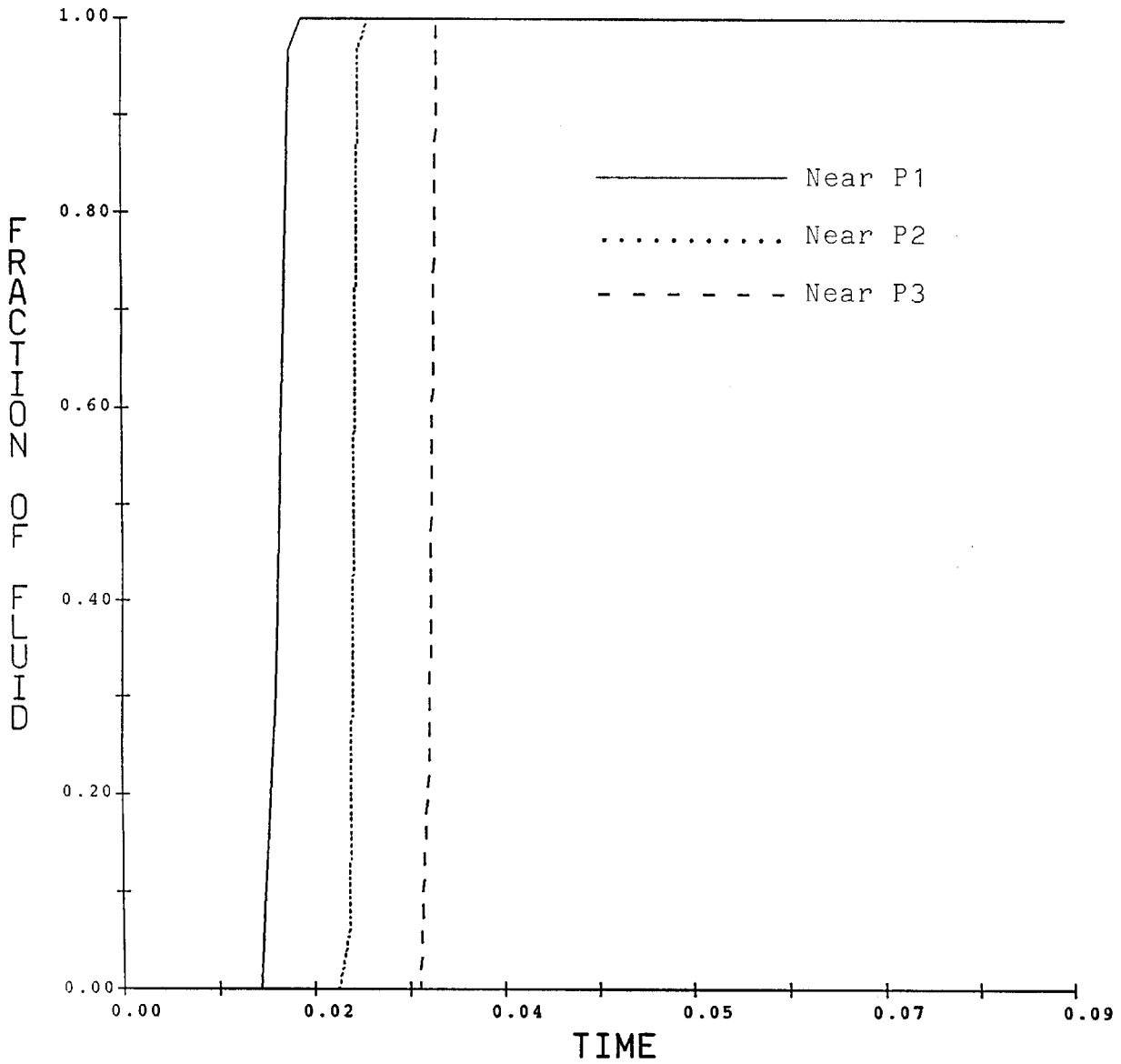
# PRESSURE COMPARISON



HYDR3D 12:26:25 6-JAN-89 OMDX VERSION 3, MOD 1, MVX 1988 X1= 2 X2= 2 X3= 24  
 CRASH SLOSH - 75% - 35 G SINUSOID ACCELERATION - INVISID

Fig. 7. Static Fluid Pressures at P1, P2, P3 for 75% Fill Case.

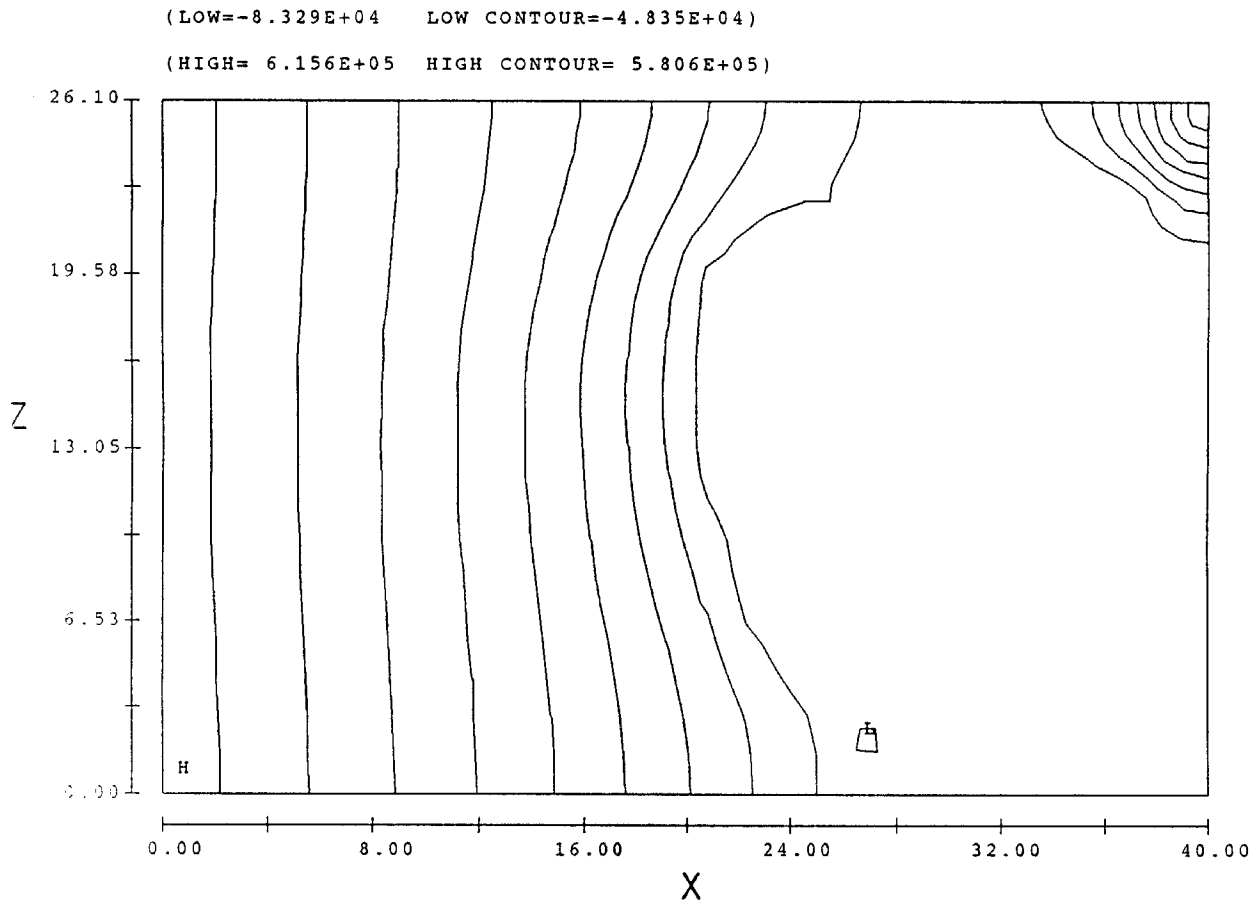
# FLUID FRACTION COMPARISON



HYDR3D 17:36:14 6-JAN-89 FVNN VERSION 3, MOD 1, MVX 1988 X1= 2 X2= 2 X3= 24  
CRASH SLOSH - 100% - 35 G SINUSOID ACCELERATION - INVISID

Fig. 8. Fluid Fractions at P1, P2, P3 for 100% Fill Case.

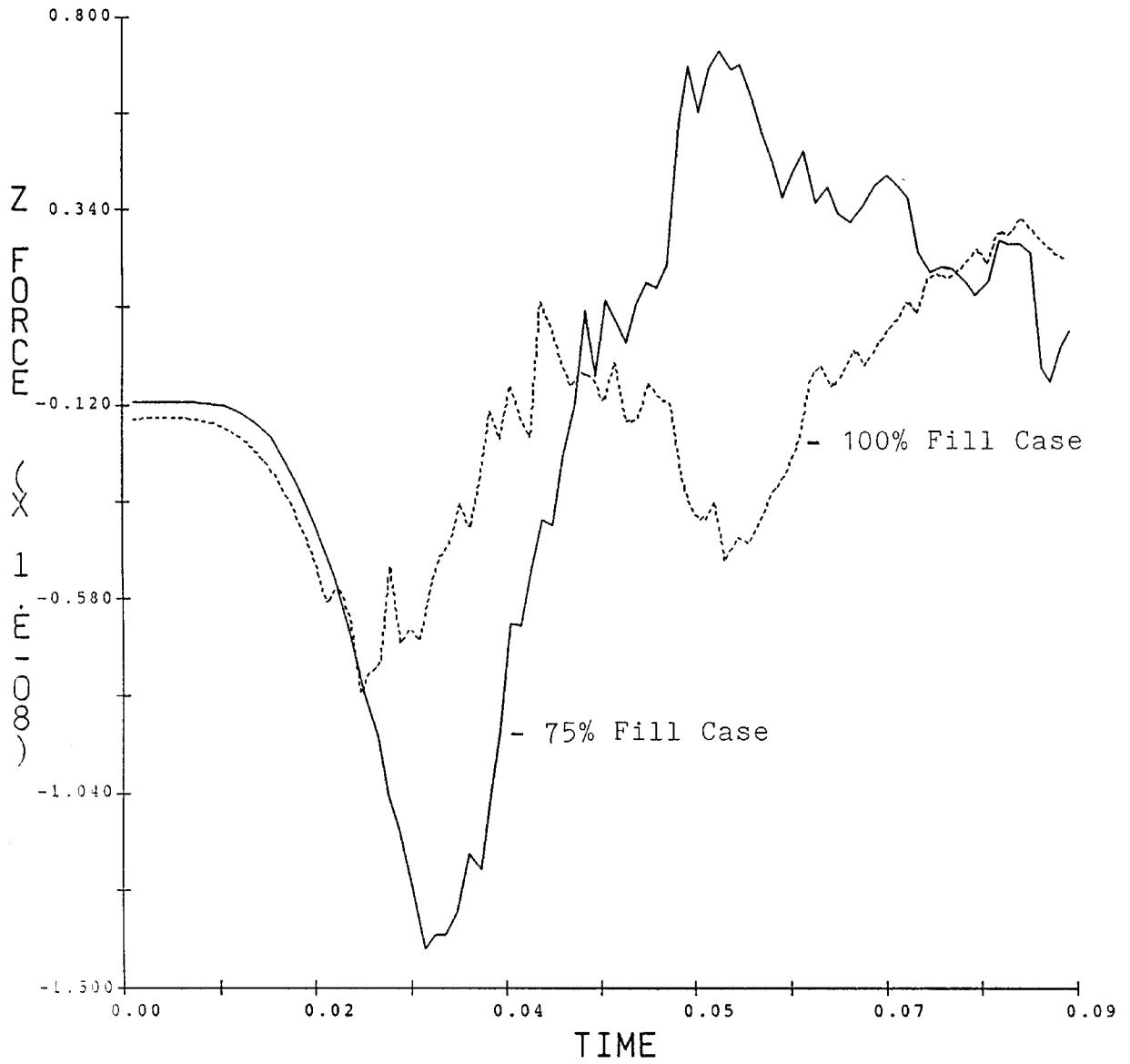
# PRESSURE CONTOURS



HYDR3D    12:26:25    6-JAN-89 OMDX    VERSION 3, MOD 1,    MVX 1988    TIME= 6.243E-02    X2= 2  
CRASH SLOSH - 75% - 35 G SINUSOID ACCELERATION - INVISID

Fig. 9. Pressure Distribution at  $t=62.4$  ms for 75% Fill Case.

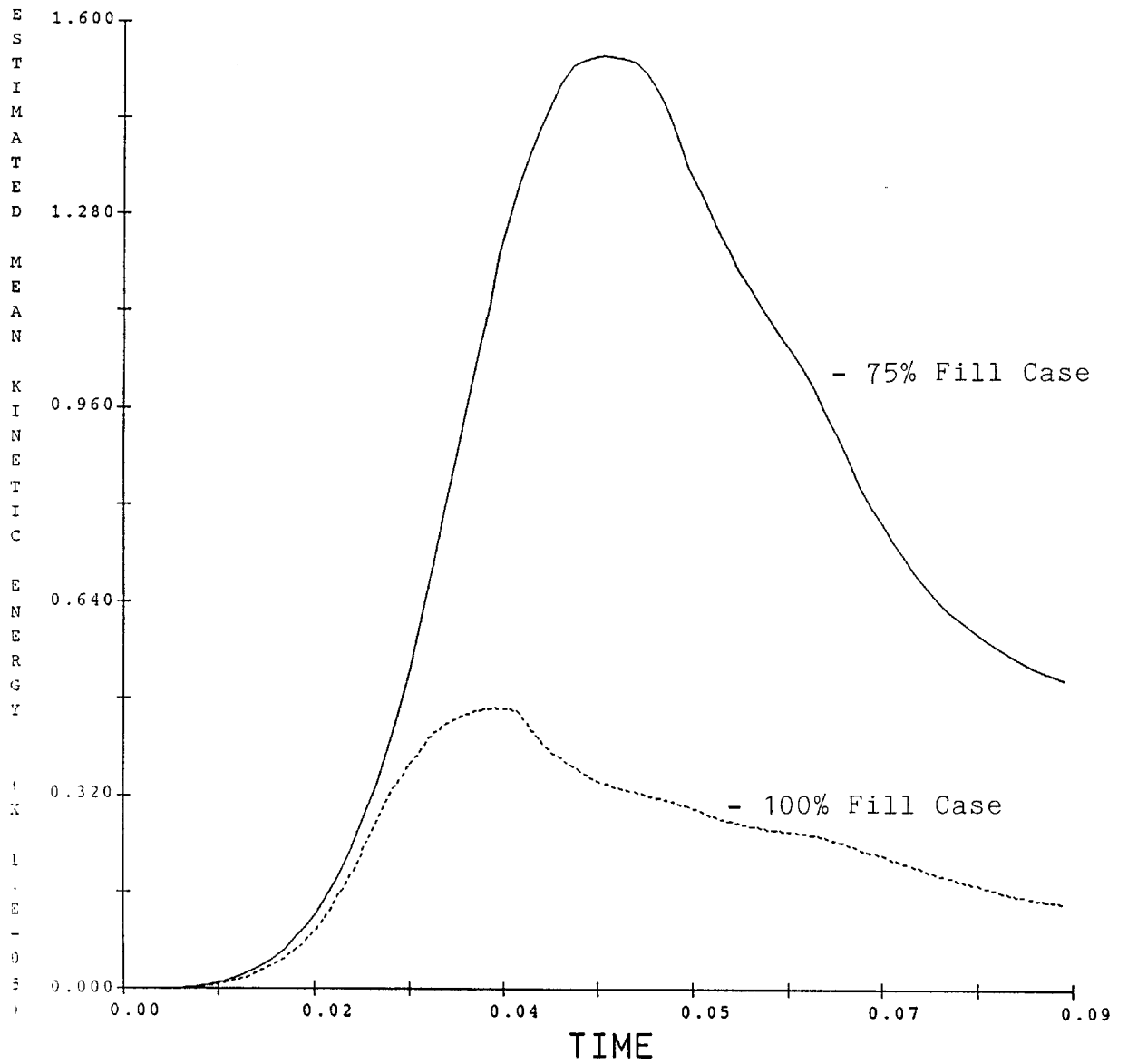
# Z FORCE COMPONENT



HYDR3D 12:26:25 6-JAN-89 OMDX VERSION 3, MOD 1, MVX 1988  
CRASH SLOSH - 75% - 35 G SINUSOID ACCELERATION - INVISID

Fig. 10. Z-Component Force Comparison

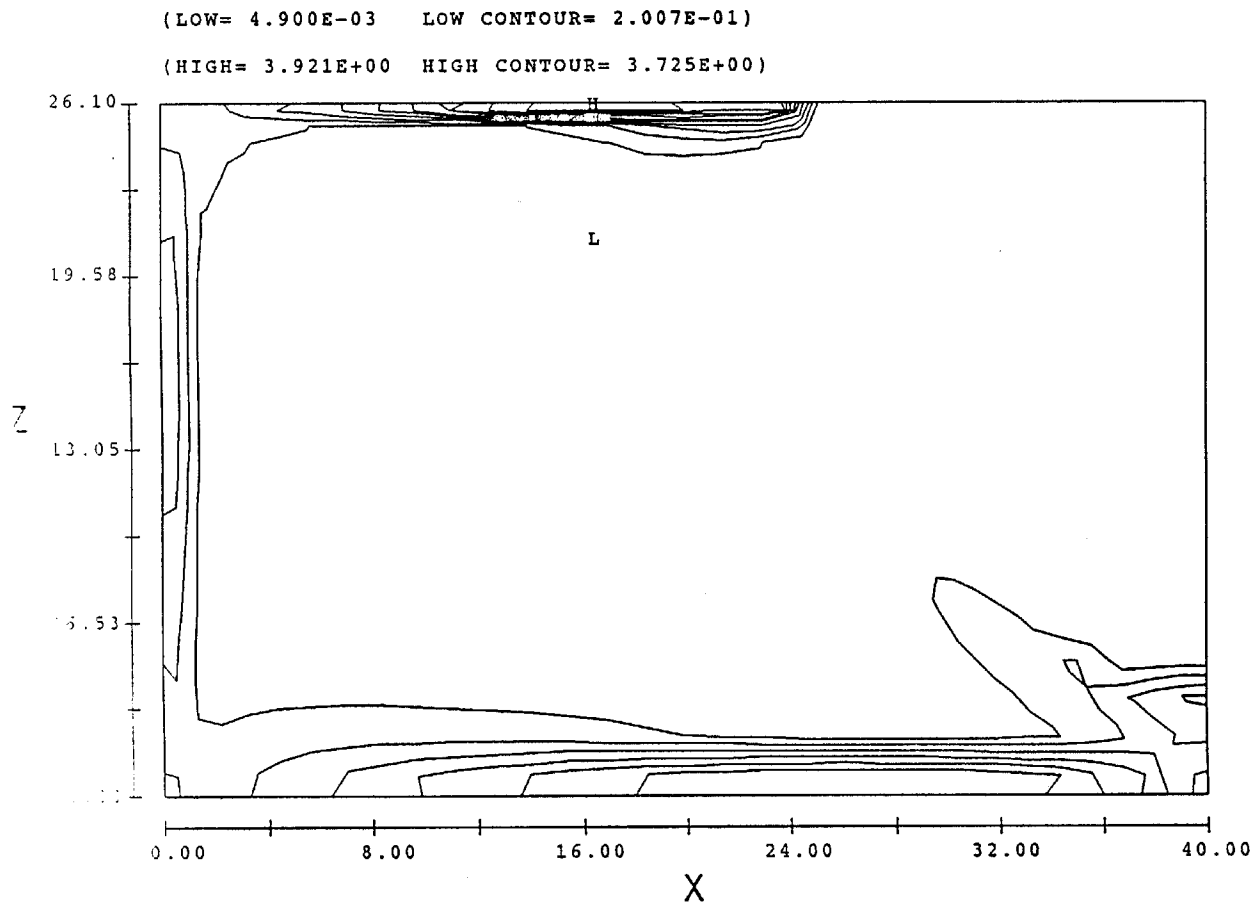
# ESTIMATED MEAN KINETIC ENERGY



HYDR3D 12:26:25 6-JAN-89 OMDX VERSION 3, MOD 1, MVX 1988  
CRASH SLOSH - 75% - 35 G SINUSOID ACCELERATION - INVISID

Fig. 11. Comparison of Fluid Kinetic Energy.

# DYNAMIC VISCOSITY CONTOURS

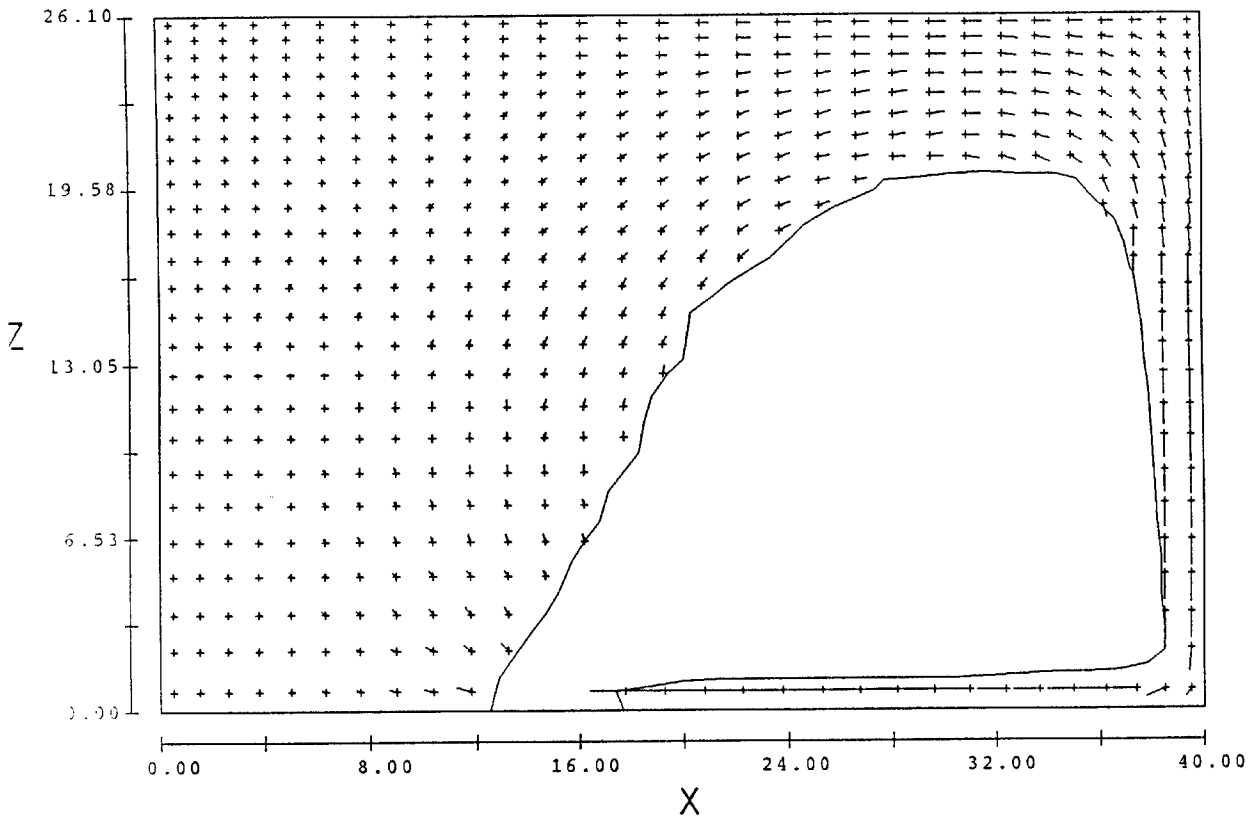


HYDR3D    17:21:02    11-JAN-89    QLQX    VERSION 3, MOD 1,    MVX 1988    TIME= 4.222E-02    X2= 2  
CRASH SLOSH - 75% - 35 G SINUSOID ACCELERATION - TURBULENT

Fig. 12. Dynamic Viscosity Distribution for k- $\epsilon$  Turbulence Model Simulation.

# VELOCITY VECTORS

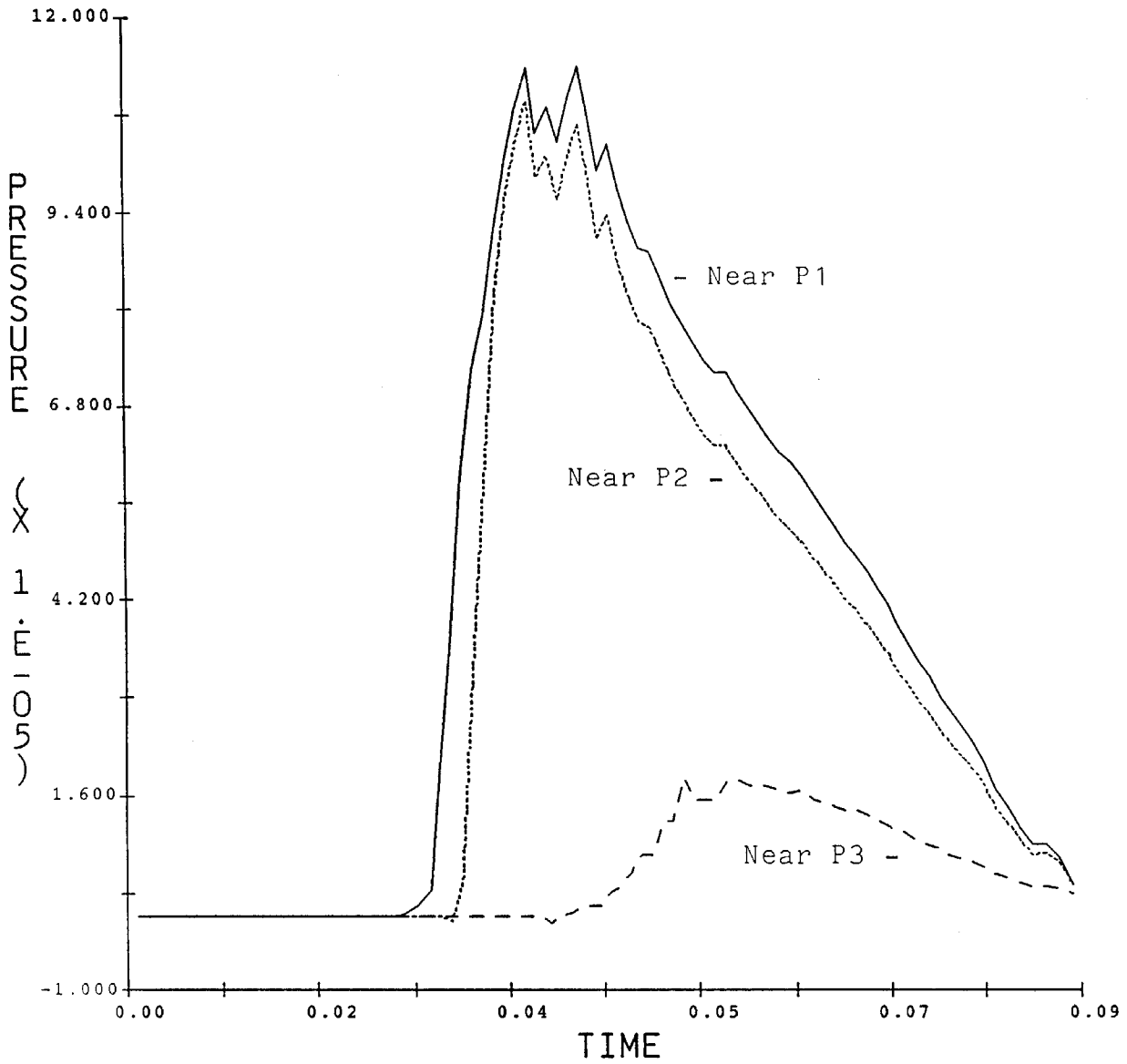
( $\leftarrow$  =  $1.02E+03$ )



HYDR3D 17:21:02 11-JAN-89 QLQX VERSION 3, MOD 1, MVX 1988 TIME= 9.016E-02 X2= 2  
CRASH SLOSH - 75% - 35 G SINUSOID ACCELERATION - TURBULENT

Fig. 13. Velocity and Fluid Distribution at  $t=90.2$  ms for  $k-\epsilon$  Turbulence Model Simulation.

# PRESSURE COMPARISON



HYDR3D 17:21:02 11-JAN-89 QLQX VERSION 3, MOD 1, MVX 1988 X1= 2 X2= 2 X3= 24  
 CRASH SLOSH - 75% - 35 G SINUSOID ACCELERATION - TURBULENT

Fig. 14. Static Fluid Pressures at P1, P2, P3 for k-ε Turbulence Model Simulation.